Canadian Science Publishing

ARTICLE

Drone Syst. Appl. Downloaded from cdnsciencepub.com by LINKOPINGS UNIVERSITETSBIBLIOTEK on 09/06/22
For personal use only.

Non-redundant high-integrity position estimation robust to sensor bias jumps using MGLR

Gustav Öman Lundin, Philippe Mouyon, Augustin Manecy, and Gustaf Hendeby

Abstract: This paper presents and experimentally evaluates an algorithm named Multiple Generalized Likelihood Ratio (MGLR) for detecting and estimating multiple consecutive measurement biases appearing frequently, in the case of non-redundant sensors; typically the case for a small drone or remotely piloted aerial vehicle. The algorithm itself is based on the Generalized Likelihood Ratio (GLR) algorithm by Willsky for bias detection and estimation, and introduces additional steps for continuously estimating, compensating, and eliminating measurement biases after detection. An experimental campaign using a car-mounted IMU and GNSS receiver in an urban environment shows the effectiveness of the approach to increase accuracy, consistency, and integrity of the estimate in non-redundant estimation with position measurements subject to time-varying bias.

Key words: position estimation, GLR, non-redundant measurements, integrity.

Résumé : Cet article présente et évalue expérimentalement un algorithme nommé « multiple generalized likelihood ratio » (rapport de vraisemblance généralisé multiple, « MGLR ») pour détecter et estimer de multiples biais de mesure consécutifs apparaissant fréquemment, dans le cas de capteurs non redondants, généralement le cas d'un petit véhicule aérien sans pilote (UAV). L'algorithme lui-même est basé sur l'algorithme du rapport de vraisemblance généralisé (« GLR ») de Willsky pour la détection et l'estimation des biais, et introduit des étapes supplémentaires pour estimer, compenser et éliminer les biais de mesure après la détection. Une campagne expérimentale utilisant un récepteur unité de mesure inertielle (IMU) et système mondial de navigation par satellite (GNSS) monté sur une voiture dans un environnement urbain montre l'efficacité de l'approche pour accroître la précision, la cohérence et l'intégrité de la valeur estimée dans l'estimation non redondante avec des mesures de position sujettes à un biais variant avec le temps. [Traduit par la Rédaction]

Mots-clés : estimation de position, rapport de vraisemblance généralisé (« GLR »), mesures non redondantes, intégrité.

1. Introduction

Navigation for drones often depends on non-redundant position sensors, such as Global Navigation Satellite System (GNSS) receivers or vision sensors. The obvious problem that arises is that sensor biases directly impact the accuracy of the position estimate. Unlike large crewed aircraft, a drone has neither backup navigation systems nor a pilot that can assess the situation and reject the faulty information.

Received 18 February 2022. Accepted 24 May 2022.

G. Öman Lundin, P. Mouyon, and A. Manecy. ONERA, Toulouse, Occitanie, France.
G. Hendeby. Linköping University, Linköping, Östergötland, Sweden.
Corresponding author: Gustav Öman Lundin (e-mail: gustav.oman_lundin@onera.fr).
© 2022 The Author(s). This work is licensed under a Creative Commons Attribution 4.0 International License (CC BY 4.0), which permits unrestricted use, distribution, and reproduction in any medium, provided the original author(s) and source are credited.

Drone Syst. Appl. Downloaded from cdnsciencepub.com by LINKOPINGS UNIVERSITETSBIBLIOTEK on 09/06/22
For personal use only.

A common type of sensor faults impacting GNSS receivers and vision sensors is quasi-constant biases. In the former case (GNSS), these can be due to loss and (or) addition of one or several satellites in the solution, apparition of multipath for several satellites' signals, or switching of operation mode (e.g., transition from Satellite Based Augmentation Systems (SBAS) to single). In the latter case (vision) these can be due to, for example, image feature tracking errors. A common factor for these faults is that they cannot be assumed to be rare events for aerial vehicles operating in a complex (urban) environment.

In addition to impacting the accuracy of the consolidated, or estimated, position, these biases have a direct impact on the integrity of the position estimate. Either the sensors are considered fault-free, and all faults violate this assumption, or the sensors are potentially faulty, and the unknown fault estimate must be accounted for.

To safeguard the accuracy and integrity of the position estimate one must therefore apply methods capable of detecting and estimating quasi-constant biases appearing frequently. At the same time, the integrity of the estimate must be handled to avoid untimely mission interruptions.

The main problem of detecting and estimating biases in non-redundant sensor suits is that the biases are only observable during a limited time after apparition. In the linear time invariant case, such as position estimation, this can easily be seen by studying the observability Gramian. The problem is therefore to detect the appearance time of the bias to properly estimate it.

An important aspect of position estimation is the integrity of the estimated position. If the position sensors are considered fault free, the integrity (through the protection level) is simply proportional to the uncertainty of the estimate. In the case where the position sensors are considered potentially biased, the uncertainty of the bias estimation also enters into the calculation of the integrity. It is therefore important to assess this uncertainty and also to be able to determine the absence of bias to guarantee high integrity over time.

Following the above points, any method for high-integrity non-redundant position estimation needs to:

1. detect and estimate multiple biases appearing frequently on non-redundant position sensors;
2. assess the integrity impact due to bias detection and estimation; and
3. detect the absence of bias on the measurement for maintained integrity over time.

1.1. State of the art

The Generalized Likelihood Ratio Test (GLRT) is conceptually a generalisation of the likelihood ratio test (LRT), where the simple fault hypothesis of a fixed fault amplitude is replaced by a composite hypothesis with a variable fault amplitude (van Trees 2001): a least squares (LS) estimate of the fault amplitude at each instant of the monitored sequence.

The GLR *algorithm*, originally proposed by Willsky (Willsky and Jones 1974; Willsky 1976), is a combination of a Kalman filter designed under the hypothesis of no fault (H_0), and a bank of LS estimators, to which is applied a GLRT to find a maximum likelihood estimate of the fault time, k, and amplitude, $\boldsymbol{b}$. In case a fault is declared by the GLRT, these estimates are used to correct the state of the Kalman filter. The GLR algorithm fundamentally consists of a linearly growing bank of LS filters. When implemented online, the filter bank is truncated to a constant number of filters on a sliding window where a single bias appearing in the observation window is considered. This obviously poses a problem when bias changes appear frequently, which can often be the case for GNSS in urban navigation (Zhu et al. 2018). Some attempts to remedy this problem have been proposed (Jamouli and Sauter 2008; Jamouli et al. 2012) in the form of an active GLR algorithm (in the sense of continuous

Drone Syst. Appl. Downloaded from cdnsciencepub.com by LINKOPINGS UNIVERSITETSBIBLIOTEK on 09/06/22
For personal use only.

bias estimation) for fault tolerant control systems, and (Xu and Li 2007) for MIMO (multi-input multi-output) radar tracking. In both these cases, the problem is treated in an entirely sequential way, meaning that only the last appearing bias is continuously estimated.

Despite its widespread use as a detector, the GLR algorithm has received criticism for being limited to Gaussian noise models and linear or quasi-linear systems (Kerr 2006). In response to this criticism, further developments of the GLR have been proposed to counter nonlinearities and non-Gaussian noise. In Faurie and Giremus (2010), a detector combining GLR and M-estimation is proposed to detect and estimate range biases, whereas in Liu and Zhong (2014) a nonlinear version of the GLR is proposed and applied to a fault-tolerant flight control system.

The GLR algorithm has found use in, among other applications, GNSS receiver bias detection (Faurie and Giremus 2010), inertial navigation (Palmqvist 1996), radar target tracking (Gao et al. 2016), and fault tolerant attitude estimation (Pirmoradi et al. 2009). In many uses of the GLR algorithm, only the detection part is used, the GLR test (GLRT), and no attention is given to the detected amplitude. Furthermore, biases are considered to be rare events, thus the single bias hypothesis of the GLR is a valid assumption.

Other methodological approaches for bias estimation based on Kalman filtering have also been proposed. Lu et al. (2015) used an aircraft kinematic model combined with an air data sensor model that switches to alternately estimate states and biases. In Alcalay et al. (2018), the filter uses the dynamic lift equation to add redundancy for air data sensor bias estimation. Finally, in approaches such as Lesouple et al. (2019) and Jiang et al. (2022), redundancy is recovered by assuming some measurements to be free from bias, which can be true in the studied GNSS cases where some satellites have line-of-sight to the rover whereas others do not. It cannot be said generally that observability can be recovered through redundancy in all applications, which is one of the motivations behind the methods in this article.

Finally, the problem of pure position estimation using non-redundant measurements subject to frequently appearing biases is largely unattended, possibly because so far, the applications are either high-end with redundant measurements (large aircraft, GNSS receivers, autonomous vehicles), or low-end with little interest in high accuracy and integrity (small unmanned aerial vehicles (UAVs)). The state of the art also shows little interest in the integrity of the estimate in the non-redundant sensors case, the vast majority of the integrity literature stemming from the GNSS domain (implying redundant range measurements). To achieve high integrity navigation for non-redundant platforms, such as unmanned vehicles and the like. This is clearly a topic that requires additional attention.

1.2. Contributions

Our contribution in this paper is the Multi-GLR (MGLR) – an extension of the GLR algorithm – to improve the state estimate in cases of frequently occurring measurement bias jumps. The main contribution is the addition of a re-identification stage for detected bias jumps, allowing the continuous estimation of the amplitude of detected bias jumps without sacrificing the ability to detect subsequent jumps. In addition, a mechanism for reducing the drift of the corrected state estimate over time is introduced. This mechanism consists of hypothesis tests of the accumulated bias jump sequence, globally or partially, where the concerned estimated bias jumps are set to zero if the test passes. This avoids accumulating residual errors due to imperfect estimations over time, if a combination of detected biases comes close to zero. The effectiveness of these improvements of the GLR algorithm are shown in simulations and using real data from a car-mounted inertial/GNSS experimental setup.

Drone Syst. Appl. Downloaded from cdnsciencepub.com by LINKOPINGS UNIVERSITETSBIBLIOTEK on 09/06/22
For personal use only.

1.3. Paper outline

In Section 2 the non-redundant position bias estimation problem is introduced together with an introduction to the GLR algorithm in Section 3 and the idea of sequential bias detection and estimation. In Section 4 we define the MGLR algorithm for multiple sequential bias estimation. Section 5 presents three strategies for bias elimination to improve the accuracy and integrity over time. A Monte Carlo simulation is performed in Section 6 showing the effectiveness of the MGLR and the bias elimination compared to the state of the art. Section 7 shows an experimental evaluation of position estimation in an urban environment. Finally, Section 8 concludes the obtained results and proposes a way forward.

2. Estimation with biased measurements

2.1. Fault modelling

Consider the linear stochastic discrete time system ($t \geq 0$) with a vector-valued bias $\boldsymbol{b} \in \mathbb{R}^{n_b \times 1}$ appearing on the measurement at time k

$$\text{(1)} \quad \boldsymbol{x}_{t+1} = A\boldsymbol{x}_t + B\boldsymbol{u}_t + \boldsymbol{v}_{x,t} \qquad \boldsymbol{y}_{t+1} = C\boldsymbol{x}_{t+1} + F\Gamma_{t+1-k}\boldsymbol{b}_{t+1} + \boldsymbol{w}_{y,t+1}$$

where $\boldsymbol{x}_t \in \mathbb{R}^{n\times 1}$, $\boldsymbol{y}_t \in \mathbb{R}^{m\times 1}$, $\boldsymbol{u}_t \in \mathbb{R}^{p\times 1}$, $\boldsymbol{b}_t \in \mathbb{R}^{n_b\times 1}$, $A \in \mathbb{R}^{n\times n}$, $B \in \mathbb{R}^{n\times p}$, $C \in \mathbb{R}^{m\times n}$, and $F \in \mathbb{R}^{m\times n_b}$. The process and output noise are $\boldsymbol{v}_{x,t} \sim \mathcal{N}(0,Q) \in \mathbb{R}^{n\times 1}$ and $\boldsymbol{w}_{y,t+1} \sim \mathcal{N}(0,R) \in \mathbb{R}^{m\times 1}$, where $Q \in \mathbb{R}^{n\times n} \geq 0$ and $R \in \mathbb{R}^{m\times m} > 0$. This system representation is typical for the problem of translational position kinematics, where acceleration or speed measurements expressed in an inertial frame are used as inputs and position measurements (e.g., GNSS measurements) are expressed in the same frame, in which case we get the classical linear double-integrator.

The function Γ_{t-k} is the output *fault signature*, representing the appearance of measurement bias at time $t = k$. The signature of a constant bias vector is modelled as $\Gamma_{t-k} = IY_{t-k}$, and for a drift it is $\Gamma_{t-k} = (t-k)Y_{t-k}\Delta t$, where Y_{t-k} is Heaviside's step function. F is the fault distribution matrix indicating which measurements are subject to bias. Note that a single bias can affect several sensors, or different sensors can be affected by different bias. Whatever the distribution, this model assumes that the biases all appear at time k.

To force a non-redundant sensor case, the fault distribution matrix is set to $F = I$, meaning that all measurements are potentially biased. This is not a unique solution though since we can, for example, measure position and velocity, and only consider biases on the position (i.e., $F \neq I$), but still end up with a non-redundant system in terms of the position.

2.2. Observability

If no bias can be found, the observability of the nominal system (1) is given by the pair (A, C). It is assumed to be fulfilled. If a bias can exist and must be estimated, it can be integrated in the state vector, we obtain the *augmented system* defined by the matrices A', B', C' as follows:

$$\text{(2)} \quad \begin{pmatrix} \boldsymbol{x} \\ \boldsymbol{b} \end{pmatrix}_{t+1} = \overbrace{\begin{pmatrix} A & 0 \\ 0 & I \end{pmatrix}}^{A'} \begin{pmatrix} \boldsymbol{x} \\ \boldsymbol{b} \end{pmatrix}_t + \overbrace{\begin{pmatrix} B \\ 0 \end{pmatrix}}^{B'} \boldsymbol{u}_t + \begin{pmatrix} \boldsymbol{v}_{x,t} \\ \boldsymbol{v}_{b,t} \end{pmatrix} \qquad \boldsymbol{y}_{t+1} = \underbrace{(CF\Gamma_{t+1-k})}_{C'} \begin{pmatrix} \boldsymbol{x} \\ \boldsymbol{b} \end{pmatrix}_{t+1} + \boldsymbol{w}_{y,t+1}$$

This augmented system is uniformly observable for a known k and with redundant measurements. Then a Kalman filter can be designed to estimate $\boldsymbol{x}$ and $\boldsymbol{b}$; however, with non-redundant measurements, the system is not uniformly observable, and the filter will diverge.

A Kalman filter, or any unbiased estimator, based on the system (1) will produce a biased state estimate if a bias appears on a non-redundant measurement (Pei et al. 2019). A typical

Fig. 1. INS/GNSS Kalman filter response to a GNSS measurement bias.

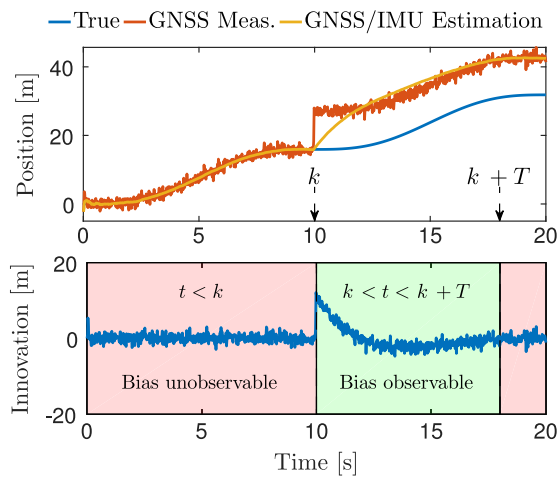

response of a position estimation Kalman filter (position estimate $\hat{\boldsymbol{x}}$, innovation $\boldsymbol{\nu}$) to the appearance of bias on the measurement of a non-redundant position sensor takes the form of Fig. 1.

It is clear from the Kalman filter response that the bias is observable during a limited time T, which is the length of the transient (see Fig. 1) and depends on the observer gains. Although not uniformly observable, the system is observable for $k < t < k + T$ if k is known.

2.3. Superposition and fault signatures

When a bias appears on a measurement with white noise, the measurement error becomes coloured noise. To estimate the bias, it is intuitive to pose the problem as a superposition of a nominal part, where only the stochastic uncertainty (white noise) applies, and a faulty part where the effect of the bias appears (Willsky and Jones 1974), that is,

$$\begin{aligned} \boldsymbol{x}_t &= \boldsymbol{x}_t^{\mathrm{n}} + \boldsymbol{x}_t^{\mathrm{f}} \\ \boldsymbol{y}_t &= \boldsymbol{y}_t^{\mathrm{n}} + \boldsymbol{y}_t^{\mathrm{f}} \end{aligned} \quad \text{with} \quad \begin{aligned} \boldsymbol{x}_{t+1}^{\mathrm{f}} &= 0 \\ \boldsymbol{y}_{t+1}^{\mathrm{f}} &= F\Gamma_{y,t+1-k}\boldsymbol{b} \end{aligned} \tag{3}$$

where n corresponds to the nominal stochastic dynamics and f to the deterministic fault effect. Furthermore, a Kalman filter, based on the hypothesis of white noise, can be applied to estimate the fault-free state ($\hat{\boldsymbol{x}}_t^{\mathrm{n}} \sim \mathcal{N}(\boldsymbol{x}_t^{\mathrm{n}}, P_t)$) using a classical recursion

$$\begin{array}{ll} \text{Prediction} & \text{Correction} \\ \hat{\boldsymbol{x}}_{t+1}^{+} = A\hat{\boldsymbol{x}}_t + B\boldsymbol{u}_t & \hat{\boldsymbol{x}}_{t+1} = \hat{\boldsymbol{x}}_{t+1}^{+} + K_{t+1}\boldsymbol{\nu}_{t+1} \\ P_{t+1}^{+} = AP_tA^{\mathrm{T}} + Q & P_{t+1} = [I - K_{t+1}C]P_{t+1}^{+} \end{array} \tag{4}$$

The prediction error $\boldsymbol{\nu}$, called the *innovation*, its covariance S, and the correction gain K are calculated as

$$\boldsymbol{\nu}_{t+1} = y_{t+1} - C\hat{\boldsymbol{x}}_{t+1}^{+} \qquad S_{t+1} = CP_{t+1}^{+}C^{\mathrm{T}} + R \qquad K_{t+1} = P_{t+1}^{+}C^{\mathrm{T}}S_{t+1}^{-1} \tag{5}$$

Using this recursion, the response of a Kalman filter based on the fault-free system at the occurrence of a bias on the measurement can be calculated. This response is commonly called the *fault signatures* of the state and the innovation, denoted $\Phi_{t,k}$ and $\phi_{t,k,}$ respectively.

Drone Syst. Appl. Downloaded from cdnsciencepub.com by LINKOPINGS UNIVERSITETSBIBLIOTEK on 09/06/22
For personal use only.

Drone Syst. Appl. Downloaded from cdnsciencepub.com by LINKOPINGS UNIVERSITETSBIBLIOTEK on 09/06/22
For personal use only.

Again thanks to linearity of the Kalman filter, the fault effect can be separated from the unbiased estimation

$$(6)\quad \begin{aligned} \hat{\boldsymbol{x}}_{t+1} &= \hat{\boldsymbol{x}}^{\mathrm{n}}_{t+1} + \hat{\boldsymbol{x}}^{\mathrm{f}}_{t+1} \\ \boldsymbol{\nu}_{t+1} &= \boldsymbol{\nu}^{\mathrm{n}}_{t+1} + \boldsymbol{\nu}^{\mathrm{f}}_{t+1} \end{aligned} \quad \text{with} \quad \begin{aligned} \hat{\boldsymbol{x}}^{\mathrm{f}}_{t+1} &= \Phi_{t+1,k}\boldsymbol{b} \\ \boldsymbol{\nu}^{\mathrm{f}}_{t+1} &= \phi_{t+1,k}\boldsymbol{b} \end{aligned}$$

The fault signatures can be calculated recursively as

$$(7)\quad \begin{aligned} \Phi_{t+1,k} &= A\Phi_{t,k} + K_{t+1}\phi_{t+1,k} \\ \phi_{t+1,k} &= FY_{t+1-k} - CA\Phi_{t,k} \end{aligned} \qquad \Phi_{t+1,k} \in \mathbb{R}^{n\times n_b}, \phi_{t+1,k} \in \mathbb{R}^{m\times n_b}$$

with $\Phi_{k,k} = \mathbf{0}$. Note especially that the innovation is written

$$(8a)\quad \boldsymbol{\nu}_{t+1} = \phi_{t+1,k}\boldsymbol{b}_{t+1} + \boldsymbol{w}_{\nu,t+1}$$

where $\boldsymbol{w}_{\nu,t+1} = \boldsymbol{\nu}^{n}_{t+1}$ is Gaussian zero-mean in the absence of bias, with time-varying covariance matrix S_{t+1}. An estimate of the bias can be calculated if the appearance time, k, of the bias is known, since the fault signature $\phi_{t+1,k}$ can then be calculated deterministically.

If the innovation noise is zero, this estimate is easily calculated by inverting eq. (8*a*). If the noise is significant, or the bias amplitude small, it is appropriate to calculate a LS estimate over a sliding observation window of length L, $\mathcal{O}^{L}_{t+1} = \{t+2-L, \ldots, t+1\}$, that is, solve

$$(8b)\quad [\boldsymbol{\nu}]^{L}_{t+1} = [\phi_k]^{L}_{t+1}\boldsymbol{b}_{t+1} + [\boldsymbol{w}_{\nu}]^{L}_{t+1}$$

The bracket notation represents the respective quantities in the entire observation window, that is,

$$[\boldsymbol{\nu}]^{L}_{t} = \begin{pmatrix} \boldsymbol{\nu}_t \\ \vdots \\ \boldsymbol{\nu}_{t+1-L} \end{pmatrix} \qquad [\phi_k]^{L}_{t} = \begin{pmatrix} \phi_{t,k} \\ \vdots \\ \phi_{t+1-L,k} \end{pmatrix} \qquad [\boldsymbol{w}]_t = \begin{pmatrix} \boldsymbol{w}_{\nu,t} \\ \vdots \\ \boldsymbol{w}_{\nu,t+1-L} \end{pmatrix}$$

The covariance matrix S_t can be used to scale the LS estimate. Since the estimation of $\boldsymbol{b}$ can only be done deterministically once k is known, we say that $\boldsymbol{b}$ is *conditionally estimated* on k. To estimate $\boldsymbol{b}$ we therefore first need to estimate k. Methods for determining k fall under the category of *change detection*, an overview of which can be found in Gustafsson (2000).

2.4. Accuracy, consistency, and integrity

The *estimation error* is defined as $\boldsymbol{\varepsilon}_t \triangleq \boldsymbol{x}_t - \hat{\boldsymbol{x}}_t$. Given that $\hat{\boldsymbol{x}}_t$ is unbiased, $\boldsymbol{\varepsilon}_t \sim \mathcal{N}(0, P_t)$. The estimated covariance P_t is used to calculate the *protection level*, PL, which represents the maximum estimation error given an *integrity risk* P_{ir}. That is, the minimum PL that satisfies

$$(9)\quad P(|\varepsilon| > \mathrm{PL}) \leq P_{\mathrm{ir}}$$

The protection level should be bounded by the *alert limit*, AL, which is the PL found at equality in eq. (9) (i.e., the largest admissible error without emitting an integrity alarm). See Supplementary Data[1] for details on how to calculate PL.

Three criteria are important to evaluate the estimation error: *accuracy*, *consistency*, and *integrity*.

[1]Supplementary data are available with the article at https://doi.org/10.1139/dsa-2022-0010.

Drone Syst. Appl. Downloaded from cdnsciencepub.com by LINKOPINGS UNIVERSITETSBIBLIOTEK on 09/06/22
For personal use only.

- *Accuracy*: The estimation error $\boldsymbol{\varepsilon}$ and the estimated covariance P should be as small as possible.
- *Consistency*: The estimated error covariance should reflect the covariance of the estimation error ($\mathrm{cov}(\boldsymbol{\varepsilon}) \leq P$).
- *Integrity*: The protection level is inferior to the alert limit (PL < AL).

The algorithms in this paper will be evaluated in light of these three criteria.

3. GLR algorithm for bias estimation

One change detection method, which doubles as a bias estimation algorithm, is the GLR algorithm (Willsky and Jones 1974). This algorithm handles the bias detection and estimation simultaneously by matching a bank of fault signatures against a Kalman filter innovation sequence using a bank of regressors, *fault signatures*, and LS filters, each of which assumes the appearance of a bias at a different time $k \in \{0,t\}$.

3.1. Principle

In its online implementation, the number of filters is not linearly growing with time but limited to covering the sliding observation window $\mathcal{O}_{t+1}$. In discrete applications, L is usually defined as the number of measurement samples during the observable period T, but can be chosen to be lower for computational purposes.

The principle of the online GLR algorithm (Willsky and Jones 1974; Gustafsson 2000) is as follows:

- Estimate the biased state using a Kalman filter under the hypothesis "H_0: No bias on measurement", i.e., $[\boldsymbol{\nu}]_{t+1}^{L} = [\boldsymbol{w}_\nu]_{t+1}^{L}$.
- Calculate L estimates of the bias $\hat{\boldsymbol{b}}_{t+1}$, using a bank of L LS-filters, each under a hypothesis "H_k: Bias appearance at time k", i.e., eq. (8).

Each filter calculates the fault signature matrices $\Phi_{t+1,k}$ and $\phi_{t+1,k}$ using eq. (7), given a particular k. Using the innovations in the observation window $\boldsymbol{\nu}_k, k \in \mathcal{O}_{t+1}^{L}$ and the corresponding covariances S_k, a bias estimate $\hat{\boldsymbol{b}}_{t+1,k}$ and a corresponding information matrix Λ_k are calculated with

$$\hat{\boldsymbol{b}}_{t+1,k} = \hat{\boldsymbol{b}}_{t,k} + G(\boldsymbol{\nu}_{t+1} - \phi_{t+1,k}\hat{\boldsymbol{b}}_{t,k}) \quad \text{with} \quad G = \Lambda_{t+1,k}^{-1}\phi_{t+1,k}^{\mathrm{T}}S_{t+1}^{-1} \qquad \Lambda_{t+1,k} = \Lambda_{t,k} + \phi_{t+1,k}^{\mathrm{T}}S_{t+1}^{-1}\phi_{t+1,k} \tag{10}$$

initialised using $\hat{\boldsymbol{b}}_{t,t} = \boldsymbol{0}^{n_b \times 1}$ and $\Lambda_{t,t} = \boldsymbol{0}^{n_b \times n_b}$. Note that this is also an information form of a Kalman filter based on state space model $\boldsymbol{b}_{t+1,k} = \boldsymbol{b}_{t,k}$ and eq. (8) as measurement model.

The LR statistic for each LS filter is then given by

$$l_{\mathrm{LR},t+1,k} = \hat{\boldsymbol{b}}_{t+1,k}^{\mathrm{T}}\Lambda_{t+1,k}\hat{\boldsymbol{b}}_{t+1,k} \tag{11}$$

This statistic is $\chi^2(n_b)$ distributed since $\hat{\boldsymbol{b}}_{t+1,k}$ is Gaussian with covariance $\Lambda_{t+1,k}^{-1}$.

- Determine the maximum likelihood estimate of the bias by maximising over the entire filter bank, that is,

$$\hat{k} = \mathrm{argmax}_k\{l_{\mathrm{LR},t+1,k}\} \qquad l_{\mathrm{GLR},t+1} = l_{\mathrm{LR},t+1,\hat{k}} \qquad \hat{\boldsymbol{b}}_{t+1} = \hat{\boldsymbol{b}}_{t+1,\hat{k}}$$

- Detect a bias (with estimated occurrence time $\hat{k}$ and amplitude $\hat{\boldsymbol{b}} = \hat{\boldsymbol{b}}_{t+1}$) if the maximum likelihood ratio l_{GLR} crosses a predefined threshold $l_{\mathrm{GLR,det}}$, noting that the test statistic under H_0 is χ^2-distributed with n_b degrees of freedom,

Drone Syst. Appl. Downloaded from cdnsciencepub.com by LINKOPINGS UNIVERSITETSBIBLIOTEK on 09/06/22
For personal use only.

Fig. 2. Principle of Willsky's GLR.

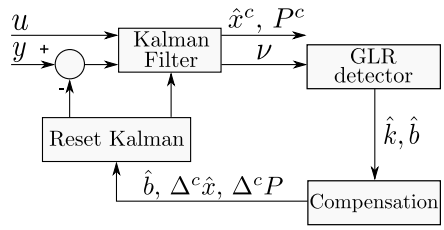

Fig. 3. Typical estimation error using GLR at the occurence of a single bias.

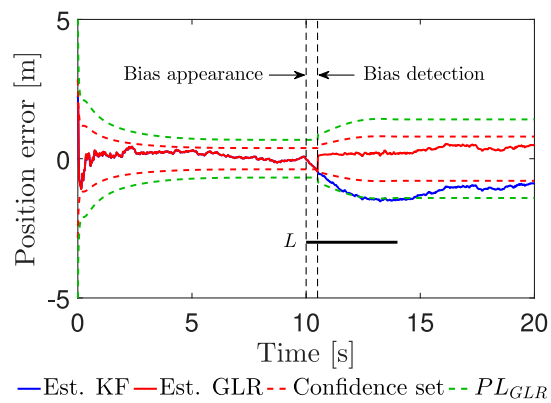

(12) $$l_{\mathrm{GLR},t+1} \underset{\hat{\boldsymbol{b}}=\boldsymbol{0}}{\overset{\hat{\boldsymbol{b}}=\hat{\boldsymbol{b}}_{t+1}}{\gtrless}} l_{\mathrm{GLR,\,det}}$$

- Compute the corrections to the measurement, the state estimate, and its covariance matrix using the estimated bias and the related state fault signature,

(13) $$\Delta^c \boldsymbol{y}_n = F\hat{\boldsymbol{b}} \qquad \Delta^c \hat{\boldsymbol{x}}_n = \Phi_{n,\hat{k}}\hat{\boldsymbol{b}} \qquad \Delta^c P_n = \Phi_{n,\hat{k}}\Lambda^{-1}_{n,\hat{k}}\Phi^{\mathrm{T}}_{n,\hat{k}}$$

- Apply them according to a chosen correction rule.

The principle of the GLR algorithm is seen in Fig. 2. Note that the way in which the corrections are applied is not apparent from the figure. Applying the GLR algorithm to the bias sequence in Fig. 1 gives the result seen in Fig. 3 ($L = 4$ s).

The classical GLR adds the correction terms only once, when the estimated bias occurrence time leaves the observation window (i.e., at time $\hat{k} + L$), and using the bias estimated at this time

(14) $$\boldsymbol{y}_n \leftarrow \boldsymbol{y}_n - \Delta^c \boldsymbol{y}_n \qquad \hat{\boldsymbol{x}}_n \leftarrow \hat{\boldsymbol{x}}_n - \Delta^c \hat{\boldsymbol{x}}_n \qquad P \leftarrow P_n + \Delta^c P_n \quad \text{with} \quad \hat{\boldsymbol{b}} = \hat{\boldsymbol{b}}_{n,\hat{k}} \quad \text{at} \quad n = \hat{k} + L$$

This correction rule optimises the accuracy on $\hat{\boldsymbol{b}}$ by maximising the observation range of its impact on ν. However, on the range $[\hat{k}, \hat{k} + L - 1]$, the state estimate is wrong and must be corrected before being output:

Fig. 4. Multiple biases in the observation window.

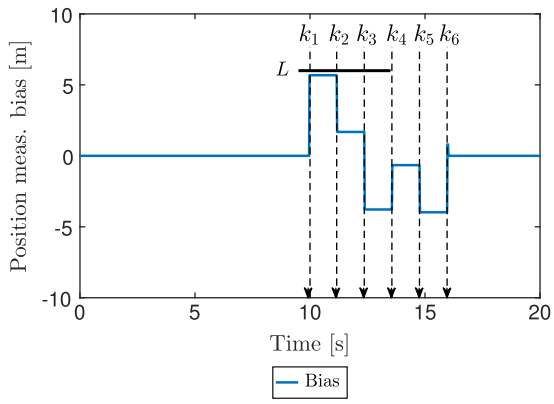

Fig. 5. A Kalman filter innovation response to multiple subsequent measurement biases.

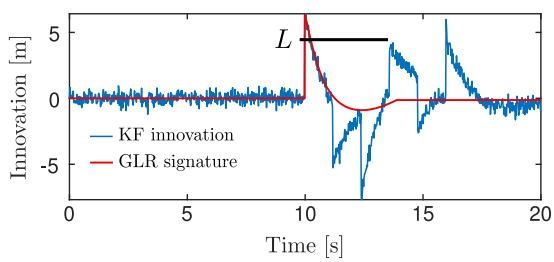

$$\hat{\boldsymbol{x}}_n^c = \hat{\boldsymbol{x}}_n - \Delta^c \hat{\boldsymbol{x}}_n \qquad P_n^c = P_n + \Delta^c P_n \quad \text{with} \quad \hat{\boldsymbol{b}} = \hat{\boldsymbol{b}}_{n,\hat{k}} \forall \hat{k} \le n < \hat{k} + L \tag{15}$$

3.2. The multi-bias case and sequential bias detection

If several biases appear in the scope of a single observation window, the classical GLR algorithm degrades since it assumes at most one bias change in the observation window (cf., Fig. 4). This degradation is trivially understood by looking at the innovation sequence of the Kalman filter (Fig. 5). In this case, the innovation can no longer be described by white noise with a signature of a single bias occurrence at time k, but is rather described by a sequence of N_b bias occurrences $\{K\} = \{k_1, \ldots, k_{N_b}\}$, that is,

$$\boldsymbol{\nu}_{t+1} = \sum_{i=1}^{N_b} \phi_{t+1,k_i} \boldsymbol{b}_{k_i} + \boldsymbol{w}_{\nu,t+1} \tag{16}$$

An ad hoc solution to this degradation was also proposed by Willsky, which is to freeze the estimation of each bias upon detection and directly apply the correction to the state and measurement. So it adds the correction terms only once, at the time of bias detection, and using the bias estimated at this date

$$\boldsymbol{y}_{t+1} \leftarrow \boldsymbol{y}_{t+1} - \Delta^c \boldsymbol{y}_{t+1} \qquad \hat{\boldsymbol{x}}_{t+1} \leftarrow \hat{\boldsymbol{x}}_{t+1} - \Delta^c \hat{\boldsymbol{x}}_{t+1} \qquad P_{t+1} \leftarrow P_{t+1} + \Delta^c P_{t+1} \quad \text{with} \quad \hat{\boldsymbol{b}} = \hat{\boldsymbol{b}}_{t+1,\hat{k}} \tag{17}$$

and obviously the filter output need not be corrected anymore. It is equal to the estimate at any time: $\hat{\boldsymbol{x}}^c = \hat{\boldsymbol{x}}$, $P^c = P$. Note this correction rule cancels out the innovation. Thus, after the

Drone Syst. Appl. Downloaded from cdnsciencepub.com by LINKOPINGS UNIVERSITETSBIBLIOTEK on 09/06/22
For personal use only.

Fig. 6. Comparison of classical GLR and ad-hoc GLR for sequential bias detection.

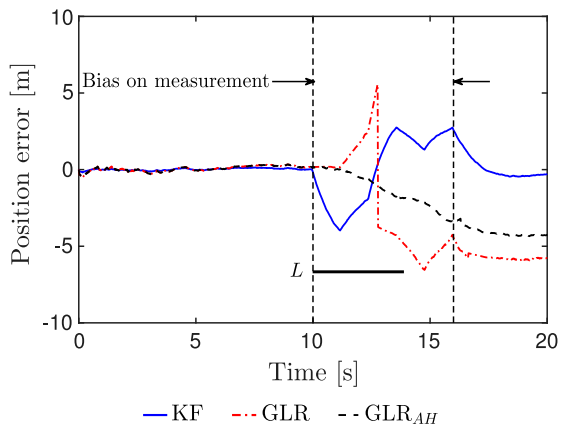

jump induced by the bias appearance, a new jump appears on the ν signal due to its compensation. An erroneous detection could be induced. This is avoided by resetting the GLR detector (i.e., the stored ν sequence is erased).

This solution has a few drawbacks, however:

1. Biases are not estimated until the end of their observability. ⇒ *Loss of accuracy.*
2. The uncertainty of each bias estimation is not properly estimated, due to point 1. ⇒ *Loss of consistency.*
3. Bias estimation errors are accumulated, thus *PL* is no longer representative of the integrity risk. ⇒ *Loss of integrity.*

An illustration of the difference between the classical GLR and the ad hoc sequential estimation GLR is seen in Fig. 6.

The ad hoc modified GLR exhibits smoother behaviour than the classical GLR in the multi-bias case since it compensates, albeit poorly over time, for the changing bias.

3.3. Active GLR algorithm

An improved solution to the ad hoc GLR, proposed in Jamouli et al. (2012) showed that a two-stage Kalman filter based on the augmented state model (2) optimally implements a sequential detection and estimation of biases from a false detection point of view. This is known as the active-GLR (AGLR).

The working principle of the AGLR is as follows:

- Predict the estimated state using a Kalman filter based on the augmented model.
- Estimate the change value of the bias state using a GLR detector (Section 3).
- If a bias change is detected, update the bias state ($\hat{\boldsymbol{b}}$) of the augmented Kalman filter with the detected amplitude and correct the predicted nominal state ($\hat{\boldsymbol{x}}$) with the corresponding fault signature. Also update the covariance P to account for the uncertainty of the bias estimation at detection.

$$\hat{\boldsymbol{b}}^{+}_{t+1} \leftarrow \hat{\boldsymbol{b}}^{+}_{t+1} + \hat{\boldsymbol{b}}_{t+1,\hat{k}} \qquad \hat{\boldsymbol{x}}^{+}_{t+1} \leftarrow \hat{\boldsymbol{x}}^{+}_{t+1} - \Phi_{t+1,\hat{k}}\hat{\boldsymbol{b}}_{t+1,\hat{k}} \qquad P^{+}_{t+1} \leftarrow P^{+}_{t+1} + \Phi_{t+1,\hat{k}}\Lambda_{t+1,\hat{k}}\Phi^{\mathrm{T}}_{t+1,\hat{k}}$$

- Correct the Kalman filter state using the updated state and covariance.

Drone Syst. Appl. Downloaded from cdnsciencepub.com by LINKOPINGS UNIVERSITETSBIBLIOTEK on 09/06/22
For personal use only.

Fig. 7. Standard deviation of estimation error for AGLR over time for 300 runs using the bias sequence in Fig. 4.

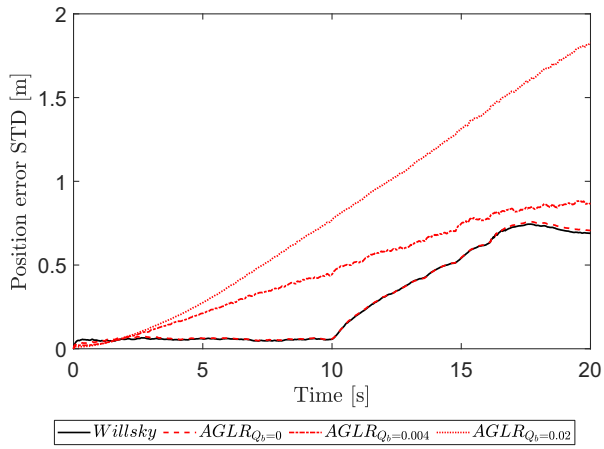

The flaw in this solution for handling measurement biases is that it is based on an augmented model, which is unobservable if the measurement is non-redundant. It thus follows that the process noise term $v_{b,t}$ should be low to limit the drift of the estimated bias $\boldsymbol{b}$ since the augmented model is unobservable for $\boldsymbol{b} \neq 0$ if k is unknown. This is contradictory to the need for a certain flexibility of the bias state to account for bad detection estimates.

A comparison between Willsky's GLR and Jamouli's AGLR is shown in Fig. 7, the bias sequence from Fig. 4 is used, with 300 different measurement and input noise sequences of equal power. As expected, the behaviour of the AGLR approximates Willsky's GLR; however, if the bias process covariance starts from zero, the unobservability of the augmented model becomes apparent.

4. MGLR algorithm

To improve the accuracy of the bias estimation compared to the one-shot bias corrections present in Willsky's GLR and the AGLR, we propose to separate the bias detection, estimation, and compensation.

The principle is simple: A GLR detector working on a corrected innovation sequence detects bias jump times. A LS estimator is then used to re-identify the bias jump amplitudes using the set of detected jump times and the uncorrected innovation from the Kalman filter. The total innovation correction calculated from the identified biases is then fed back to correct the innovation to be used for subsequent detection.

It is noteworthy that the MGLR (as well as the nominal GLR) is supposed to be triggered in steady state before faulty conditions appear (i.e., when the Kalman filter's initial convergence is done and hypothesis H_0 can be trusted). For example, in GNSS applications, in open-sky conditions and not to close to the ground. This will guarantee that the hypothesis H_0 holds when entering a degraded environment (subject to strong occlusion, multipath effects, etc.). If this cannot be achieved (detection and estimation filters started simultaneously) a large initialisation error would require an equally bloated covariance matrix P_0 for the Kalman filter in order not to detect the initial convergence as a bias (given that the subsequent measurements are coherent with the true state and not the initial state). See, for example, Lu et al. (2015).

Drone Syst. Appl. Downloaded from cdnsciencepub.com by LINKOPINGS UNIVERSITETSBIBLIOTEK on 09/06/22
For personal use only.

Drone Syst. Appl. Downloaded from cdnsciencepub.com by LINKOPINGS UNIVERSITETSBIBLIOTEK on 09/06/22
For personal use only.

4.1. Multiple bias detection

By resetting the Kalman state at each new detection, the classical GLR and the AGLR remove the effect of a bias jump on the Kalman innovation, allowing for a subsequent jump detection; however, if the Kalman filter state is not reset at detection, we can still apply a feedback compensation to the innovation using the estimated signatures of all previously detected bias jumps, that is,

$$\boldsymbol{\nu}^c_{t+1} = \boldsymbol{\nu}_{t+1} - \Delta\boldsymbol{\nu}^c_{t+1}$$

The correction term, $\Delta\boldsymbol{\nu}^c_t$, is split into a long-term correction, $\Delta\boldsymbol{\nu}^{c,\mathrm{lt}}_{t+1}$, applied for all biases no longer in the observation window, and a short term correction, $\Delta\boldsymbol{\nu}^{c,\mathrm{st}}_{t+1}$, applied for all biases still in the observation window:

$$\Delta\boldsymbol{\nu}^c_{t+1} = \underbrace{\sum_{\hat{k}_i \le t+1-L} \phi_{t+1,\hat{k}_i} \hat{\boldsymbol{b}}_{t+1,\hat{k}_i}}_{\Delta\boldsymbol{\nu}^{c,\mathrm{lt}}_{t+1}} + \underbrace{\sum_{t+1-L<\hat{k}_i \le t+1} \phi_{t+1,\hat{k}_i} \hat{\boldsymbol{b}}_{t+1,\hat{k}_i}}_{\Delta\boldsymbol{\nu}^{c,\mathrm{st}}_{t}}$$

The long-term correction is explicit here, but is implicitly handled by resetting the Kalman filter state once a detection time $\hat{k}_i$ leaves the observation window. The corrected innovation including all N_b detected bias jumps currently in the observation window is therefore written

$$\boldsymbol{\nu}^c_{t+1} = \boldsymbol{\nu}_{t+1} - \sum_{i=1}^{N_{\hat{b}}} \phi_{t+1,\hat{k}_i} \hat{\boldsymbol{b}}_{t+1,\hat{k}_i} \tag{18}$$

This corrected innovation is then used by a GLR-detector to detect a subsequent bias jump, which is then added to the set of detected bias jump times $\hat{k}_i$.

4.2. Multiple bias re-identification

The objective of the re-identification is to minimise the covariance of corrected innovation over the observation window. At any time $t+1$ we therefore have to solve a system of L linear equations to find the set of estimated bias jumps $\left\{\hat{\boldsymbol{b}}_{\hat{k}_i}\right\} = \left\{\hat{\boldsymbol{b}}_{\hat{k}_1}, \ldots, \hat{\boldsymbol{b}}_{\hat{k}_{N_{\hat{b}}}}\right\}$:

$$[\boldsymbol{\nu}]_{t+1} = \left[\phi_{\hat{k}_i}\right]_{t+1} \left[\boldsymbol{b}_{\hat{k}_i}\right]_{t+1} + \left[\boldsymbol{w}\right]_{t+1} \tag{19}$$

where the bracket notation represents the respective quantities in the entire observation window, that is,

$$[\boldsymbol{\nu}]_{t+1} = \begin{pmatrix} \boldsymbol{\nu}_{t+1} \\ \vdots \\ \boldsymbol{\nu}_{t-L+1} \end{pmatrix} \qquad \left[\phi_{\hat{k}_i}\right]_{t+1} = \begin{pmatrix} \phi_{t+1,\hat{k}_1} & \cdots & \phi_{t+1,\hat{k}_{N_{\hat{b}}}} \\ \vdots & \ddots & \vdots \\ \phi_{t-L+1,\hat{k}_1} & \cdots & \phi_{t-L+1,\hat{k}_{N_{\hat{b}}}} \end{pmatrix} \qquad \left[\boldsymbol{b}_{\hat{k}_i}\right]_{t+1} = \begin{pmatrix} \boldsymbol{b}_{t+1,\hat{k}_1} \\ \vdots \\ \boldsymbol{b}_{t+1,\hat{k}_{N_{\hat{b}}}} \end{pmatrix} \qquad \left[\boldsymbol{w}\right]_{t+1} = \begin{pmatrix} \boldsymbol{w}_{\nu,t+1} \\ \vdots \\ \boldsymbol{w}_{\nu,t-L+1} \end{pmatrix}$$

This system is in principle easy to solve by a LS estimator, the algorithm is then called MGLR-LS. For online applications, solving the above LS problem can be computationally costly, and a recursive LS method, MGLR-RLS, can be used instead. For any $\hat{k}_j$ in $\{\hat{k}_i\}$, the recursion is given by

$$\hat{\boldsymbol{b}}_{t+1,\hat{k}_j} = \hat{\boldsymbol{b}}_{t,\hat{k}_j} + G\left(\nu_t - \sum_{i=1}^{N_{\hat{b}}} \phi_{t+1,\hat{k}_i} \hat{\boldsymbol{b}}_{t,\hat{k}_i}\right) \qquad G = \Lambda^{-1}_{t+1,\hat{k}_j} \phi^{\mathrm{T}}_{t+1,\hat{k}_j} S_t^{-1} \qquad \Lambda_{t+1,\hat{k}_j} = \Lambda_{t,\hat{k}_j} + \phi^{\mathrm{T}}_{t+1,\hat{k}_j} S_t^{-1} \phi_{t+1,\hat{k}_j} \tag{20}$$

This recursion is initialised with the detected bias $\hat{\boldsymbol{b}}_{\mathrm{det}}$ given by the GLR detector.

After having identified all detected biases in the observation window, the predicted correction for the innovation is calculated as per eq. (18). And a subsequent bias jump can be detected.

Note that the total estimated bias in the observation window is in turn the sum of the estimated bias vector, that is,

$$\hat{\boldsymbol{b}}_{t+1} = \sum_{i=1}^{N_{\hat{b}}} \hat{\boldsymbol{b}}_{t+1,\hat{k}_i} \tag{21}$$

whereas the total observed bias on the measurement also adds the accumulated bias estimates having left the observation window:

$$\hat{\boldsymbol{b}}_{t+1,\sum} = \hat{\boldsymbol{b}}_{t+1} + \underbrace{\sum_{\hat{k}_i \le t+1-L} \hat{\boldsymbol{b}}_{t+1,\hat{k}_i}}_{\hat{\boldsymbol{b}}_{\mathrm{acc}}} \tag{22}$$

4.3. Corrected state and its covariance

Once a single bias is detected and its appearance time estimated, the appropriate corrections to find the unbiased state estimate are calculated as

$$\Delta\hat{\boldsymbol{x}}^c_{t+1} \triangleq \Phi_{t+1,\hat{k}} \hat{\boldsymbol{b}}_{\hat{k}}$$

This gives an expression of the corrected state using eq. (6),

$$\hat{\boldsymbol{x}}_{t+1} = \hat{\boldsymbol{x}}^{\mathrm{n}}_{t+1} + \hat{\boldsymbol{x}}^{\mathrm{f}}_{t+1} - \Phi_{t+1,\hat{k}} \hat{\boldsymbol{b}}_{\hat{k}} \tag{23}$$

If the appearance time is very well estimated (i.e., we can assume $\hat{k} = k$) we get

$$\hat{\boldsymbol{x}}_{t+1} = \hat{\boldsymbol{x}}^{n}_{t+1} + \Phi_{t+1,\hat{k}} (\boldsymbol{b}_{\hat{k}} - \hat{\boldsymbol{b}}_{\hat{k}}) \tag{24}$$

The estimated covariance of this corrected state is thus given by the combination of the nominal state covariance and the covariance of the bias estimation, that is,

$$P_{t+1} \leftarrow P_{t+1} + \Phi_{t+1,\hat{k}} \Lambda^{-1}_{t+1,\hat{k}} \Phi^{\mathrm{T}}_{t+1,\hat{k}} \tag{25}$$

It follows that the total state correction of all biases in the observation window is the sum of all individual corrections, and the covariance is the accumulated covariance, that is,

$$\hat{\boldsymbol{x}}^c_{t+1} = \hat{\boldsymbol{x}}_{t+1} + \underbrace{\sum_{i=1}^{N_{\hat{b}}} \Phi_{t+1,\hat{k}_i} \hat{\boldsymbol{b}}_{t+1,\hat{k}_i}}_{\Delta^c \hat{\boldsymbol{x}}^{\mathrm{st}}} \qquad P^c_{t+1} = P_{t+1} + \underbrace{\sum_{i=1}^{N_{\hat{b}}} \Phi_{t+1,\hat{k}_i} \Lambda^{-1}_{t+1,\hat{k}_i} \Phi^{\mathrm{T}}_{t+1,\hat{k}_i}}_{\Delta^c P^{\mathrm{st}}} \tag{26}$$

When a bias jump time $\hat{k}_j$ leaves the observation window, it is no longer observed by the identifications stage and is definitely removed from the measurement vector. The state estimate and its covariance $(\hat{\boldsymbol{x}}, P)$ are also reset accordingly:

Drone Syst. Appl. Downloaded from cdnsciencepub.com by LINKOPINGS UNIVERSITETSBIBLIOTEK on 09/06/22
For personal use only.

Fig. 8. Working principle of the MGLR algorithm, changes compared to Willsky's GLR marked in the blue dashed areas.

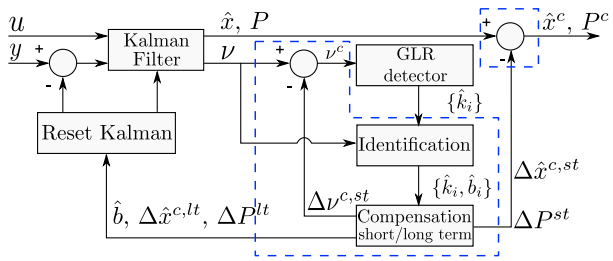

$$(27)\quad \boldsymbol{y}_m \leftarrow \boldsymbol{y}_m - F\hat{\boldsymbol{b}}_{\hat{k}_j} \qquad \hat{\boldsymbol{x}}_{t+1} \leftarrow \hat{\boldsymbol{x}}_{t+1} - \Phi_{t+1,\hat{k}_j}\hat{\boldsymbol{b}}_{t+1,\hat{k}_j} \qquad P_{t+1} \leftarrow P_{t+1} + \Phi_{t+1,\hat{k}_j}\Lambda^{-1}_{t+1,\hat{k}_j}\Phi^{\mathrm{T}}_{t+1,\hat{k}_j}$$

An overview of the MGLR working principle is shown in Fig. 8.

4.4. Tuning considerations

The parameters to tune for the MGLR algorithm are the same as for the classical GLR algorithm, that is, the observation window length, L, the detection threshold, l_{det}, and possibly a minimum detection delay, M. The window L is optimally chosen as the steady state response time of the Kalman filter, whereas $0 \le M < L$ is tuned to improve robustness to impulsive noise. If impulsive noise is not an issue, one usually takes $M = 0$. The detection threshold l_{det} is tuned with a probability of false alarm P_{FA} and is otherwise found as a standard χ_2-threshold with n_b degrees of freedom. As for any detection threshold, the lower P_{FA} the more reactive the detector is to high frequency changes; this comes at the cost of more false detection, which may lead to a drift of the corrected estimate.

4.5. Integrity of the corrected state

To evaluate the integrity of the corrected state $\hat{\boldsymbol{x}}^c$ given by the MGLR we must first assess the meaning of its covariance P^c. Indeed, P^c represents the covariance of the unbiased state estimation error plus the estimation errors of all detected and estimated bias jumps currently being observed. However, from an integrity point of view, we must also consider all $N_{\hat{b}_{\mathrm{acc}}}$ past bias jumps, having previously been detected, estimated, and corrected. Following this reasoning, the total accumulated state estimation covariance is given by

$$(28)\quad P^{\mathrm{tot}}_{t+1} = P^c_{t+1} + \sum_{i=1}^{N_{\hat{b}_{\mathrm{acc}}}} \Phi_{t+1,\hat{k}_j}\Lambda^{-1}_{t+1,\hat{k}_j}\Phi^{\mathrm{T}}_{t+1,\hat{k}_j}$$

The total number of detected biases increases monotonically, and the covariance contribution of each bias estimate is strictly positive. It follows that from an integrity point of view, the uncertainty of the corrected state can only grow over time. It is therefore necessary to apply some kind of elimination mechanism, which removes combinations of bias jumps that add up to zero, to limit the growth of the corrected state estimate error covariance over time.

This is the object of the following section.

5. Bias elimination

Intuitively one can say that in a sequence of bias jumps, adding some of them together may result in a residual jump near zero, or this may even apply to the entire sequence, as

Drone Syst. Appl. Downloaded from cdnsciencepub.com by LINKOPINGS UNIVERSITETSBIBLIOTEK on 09/06/22
For personal use only.

Drone Syst. Appl. Downloaded from cdnsciencepub.com by LINKOPINGS UNIVERSITETSBIBLIOTEK on 09/06/22
For personal use only.

in Fig. 4. This kind of behaviour is often seen in urban navigation, where multi-path effects and partial signal blocking temporarily causes shifts in the position measurement, which then disappear as soon as the obstacle (or satellite) disappears. Removing such sequences from the set of accumulated biases naturally reduces the accumulative uncertainty term in eq. (28). This process can of course be done at any moment during the estimation, but a natural point is when the most recent bias leaves the observation window. When removing only a subset of the accumulated bias set, it is called *sequential* elimination, whereas when the whole set of biases is removed it is called *global* elimination.

5.1. Accumulated bias estimation

Let us denote the set of estimated biases that have left the observation window (i.e., accumulated biases) $\{\hat{b}_{\mathrm{acc},i}\}$ and the corresponding set of information matrices $\{\Lambda_{\mathrm{acc},i}\}$. In the MGLR, once a bias leaves the observation window of the identification stage, it is added to these sets along with its information matrix. At this point, the measurement vector is also corrected by this additional bias estimation, that is,

$$\boldsymbol{y}_t^c = \boldsymbol{y}_t^{\mathrm{n}} + \boldsymbol{y}_t^{\mathrm{f}} - F\hat{\boldsymbol{b}}_{\hat{k}} = \boldsymbol{y}_t^{\mathrm{n}} + F(\boldsymbol{b}_t - \hat{\boldsymbol{b}}_{\mathrm{acc},t})$$

where the total accumulated bias and its information are given by

$$\hat{\boldsymbol{b}}_{\mathrm{acc},t} = \sum_{i=1}^{N_{\mathrm{det}}} \hat{\boldsymbol{b}}_{\mathrm{acc},i} \qquad \Lambda_{\mathrm{acc},t} = \left(\sum_{i=1}^{N_{\mathrm{det}}} \Lambda_{\mathrm{acc},i}^{-1}\right)^{-1}$$

From the correction of the measurement, we see that a badly estimated bias sequence will lead to a drift of the state estimate, since it is unbiased with respect to the biased measurement. This fact, together with the accumulated state uncertainty, is the basis of the elimination stage of the MGLR.

5.2. Global bias elimination

The conceptually simplest elimination method is to assume that when no more biases are being estimated, a test can be performed to see whether the accumulated bias sequence satisfies the hypothesis of zero-mean. If this test passes, the accumulated bias $\boldsymbol{b}_{\mathrm{acc},t}$ and its associated information matrix $\Lambda_{\mathrm{acc},t}^{-1}$ are reset to zero, in turn effectively reducing the uncertainty of the corrected state $\hat{\boldsymbol{x}}_{t+1}^c$.

The estimated accumulated bias is written as the actual accumulated bias plus the accumulated bias estimation errors (due to missed detection, finite observations, noise, etc.),

$$\hat{\boldsymbol{b}}_{\mathrm{acc},t} = \boldsymbol{b}_{\mathrm{acc},t} + \sum_{i=1}^{N_b} \epsilon_{b,i}$$

where N_b is the number of actual biases, and $\epsilon_{b,i}$ the estimation errors. Note that for a missed detection of b_j, we have $\epsilon_{b,i} = b_j$. Since we do not have access to the actual estimation errors $\{\epsilon_{b,i}\}$, we have to assume that all significant biases have been detected and that all non-detections are zero-mean. In this case, we can say that the accumulated estimation error is zero-mean with covariance $\Lambda_{\mathrm{acc},t}^{-1}$. To test the global elimination we can then assume the zero-hypothesis

$$H_0 : \hat{\boldsymbol{b}}_{\mathrm{acc},t} \sim \mathcal{N}(\boldsymbol{0}, \Lambda_{\mathrm{acc},t}^{-1})$$

which is satisfied if the accumulated estimated bias is near zero, that is, if

Drone Syst. Appl. Downloaded from cdnsciencepub.com by LINKOPINGS UNIVERSITETSBIBLIOTEK on 09/06/22
For personal use only.

(29) $\hat{\boldsymbol{b}}_{\mathrm{acc},t}^{T}\Lambda_{\mathrm{acc},t}\hat{\boldsymbol{b}}_{\mathrm{acc},t} < l_{\mathrm{GLR,\,det}}$

The tuning threshold is set as the same threshold used by the GLR detector, implying that only an accumulated bias smaller than the smallest detectable one should be eliminated. If this test is passed, the accumulated sets $\{\hat{b}_{\mathrm{acc},i}\}$ and $\{\Lambda_{\mathrm{acc},i}\}$ are set to zero. By resetting the accumulated bias estimation, the corresponding correction is removed from the measurement:

$$\boldsymbol{y}_m \leftarrow \boldsymbol{y}_m - F\hat{\boldsymbol{b}}_{\mathrm{acc}}$$

The bias $\hat{\boldsymbol{b}}_{\mathrm{acc}}$ is only approximately zero. When we reset the accumulated bias, it is as if the Kalman filter is reset with a state estimate that is slightly biased compared to the measurement. The innovation $\boldsymbol{\nu}_{t+1}$ of the subsequent iteration can therefore be slightly non-zero, that is,

$$\boldsymbol{\nu}_{t+1} = \boldsymbol{y}_{m,t+1} - C\hat{\boldsymbol{x}}_{t+1}^{+} \sim \mathcal{N}(0, CP_{t+1}^{+}C^{\mathrm{T}} + R) - F\hat{\boldsymbol{b}}_{\mathrm{acc}} \sim \mathcal{N}(-F\hat{\boldsymbol{b}}_{\mathrm{acc}}, CP_{t+1}^{+}C^{\mathrm{T}} + R)$$

To avoid a false detection due to this bias accumulation reset, the uncertainty of the accumulated (and removed) bias can be transferred to the current Kalman state covariance, P_t, that is, at the moment of resetting we set

$$P_t \leftarrow P_t + \Delta P_t$$

The term ΔP_t is found by equating the innovation covariance before and after the reset:

$$C(AP_tA^{\mathrm{T}} + Q)C^{\mathrm{T}} + R + F\Lambda_{\mathrm{acc}}^{-1}F^{\mathrm{T}} = C[A(P_t + \Delta P_t)A^{\mathrm{T}} + Q]C^{\mathrm{T}} + R$$

This gives ΔP_t as

$$\Delta P_t = (CA)^{\dagger}F\Lambda_{\mathrm{acc}}^{-1}F^{\mathrm{T}}(C^{\mathrm{T}}A^{\mathrm{T}})^{\dagger}$$

where $(.)^{\dagger}$ signifies the pseudo inverse of a matrix. Note that this compensation lacks mathematical rigour since we confuse a shift in the mean with an increased covariance; however, experience shows that it works well in practice.

It is easy to find bias sequence examples where the global bias elimination will not work very well. For example, in an urban GNSS environment where a brutal constellation change is followed by a sequence of minor multipath biases. The accumulated bias in that case will not change significantly over time; however, the uncertainty of the estimated bias accumulation will. This can then lead to a false rejection of the large initial bias jump.

5.3. Sequential bias elimination

A smoother way of eliminating biases is to see if there are any combinations of accumulated biases that add up to near-zero. Each time a bias jump leaves the observation window, we can compare it to the set of previously estimated ones. Let us denote by B_{acc} the matrix whose columns are the elements of $\{\hat{b}_{\mathrm{acc},i}\}$

(30) $B_{\mathrm{acc}} = [\hat{\boldsymbol{b}}_{\mathrm{acc},1}, \ldots, \hat{\boldsymbol{b}}_{\mathrm{acc},N_{\mathrm{acc}}}]$

The goal is to find the combination of biases previously accumulated that adds up closest to $\hat{\boldsymbol{b}}_{\mathrm{acc},t}$. This combination is $B_{\mathrm{acc}}\boldsymbol{r}$ where $\boldsymbol{r}$ is a binary vector ($\boldsymbol{r} \in \{0,1\}^{N_{\mathrm{acc}}}$). The residual bias and its covariance are

Drone Syst. Appl. Downloaded from cdnsciencepub.com by LINKOPINGS UNIVERSITETSBIBLIOTEK on 09/06/22
For personal use only.

$$\varepsilon_t(\boldsymbol{r}) = \hat{\boldsymbol{b}}_{t,\hat{k}} - B_{\text{acc}}\boldsymbol{r} \qquad \Lambda_{t,\varepsilon}^{-1}(\boldsymbol{r}) = \Lambda_{t,\hat{k}}^{-1} + \sum_{i=1}^{N_{\text{acc}}} \Lambda_{\text{acc},i}^{-1} r_i \tag{31}$$

The criterion we minimise is

$$\boldsymbol{r}^* = \min_{r\in\{0,1\}^{N_{\text{acc}}}} \left\|\varepsilon_t(\boldsymbol{r})\right\|^2 \tag{32}$$

If a non-zero solution is found, the resulting residual, $\varepsilon_t(\boldsymbol{r}^*)$, and its covariance, $\Lambda_{t,\varepsilon}^{-1}(\boldsymbol{r}^*)$, can be used as for the global bias elimination to test whether the residual is sufficiently small to be neglected:

$$\varepsilon_t^{\mathrm{T}}(\boldsymbol{r}^*)\Lambda_{t,\varepsilon}(\boldsymbol{r}^*)\varepsilon_t(\boldsymbol{r}^*) < l_{\text{GLR, det}} \tag{33}$$

If this test is passed, the corresponding biases and their information matrices are removed from $\{\hat{b}_{\text{acc},i}\}$ and $\{\Lambda_{\text{acc},i}\}$, and the measurement correction as well as the Kalman state and its covariance.

6. Monte Carlo simulation

To evaluate the added value of the MGLR compared to Willsky's GLR and the AGLR and also the presented elimination strategies, a Monte Carlo simulation was conducted. The results of the simulation are shown in Figs. 9 and 10 in the form of the position estimation error and the protection level. The underlying process is a random walk of x driven by a noise $v \sim \mathcal{N}(0,(1/3)^2)$, and measured with a noisy measurement y polluted by $w \sim \mathcal{N}(0,(1/3)^2)$,

$$x_{t+1} = x_t + v_t\Delta t, \quad x(0) = 0 \qquad y_{t+1} = x_{t+1} + w_{t+1} + Y_{t+1-k}b$$

A measurement bias sequence $\{b_{k_1},\ldots,b_{k_N}\}$ is drawn with a mean time between biases of 1 s starting at 5 s and ending at 15 s, with bias amplitudes drawn randomly from $5\sigma_{\text{w}}$ to $10\sigma_{\text{w}}$. The GLR algorithms are all tuned with an observation window of $L = 2$ s and a probability of false alarm $P_{\text{FA}} = 10^{-4}$.

To evaluate the Monte Carlo simulations, three informative numbers can be computed. The first one is the mean of error standard deviations (i.e., $\overline{\sigma}$ of the position estimation error ε), which gives a global idea of the position error of the simulation batch:

$$\overline{\sigma} \triangleq \frac{1}{M}\sum_{i=1}^{M}\left(\sqrt{\frac{1}{N}\sum_{j=0}^{N}\varepsilon_{t_j}^2}\right)$$

The second number is the integrity rate r_{int}, for lack of a better word, expressed as the percentage of time during the simulation batch when the estimation error is superior to the protection level. From an integrity point of view, this must be minimised. Clearly during this time the integrity cannot be evaluated, unless the protection level itself crosses the alert limit.

$$r_{\text{int}} \triangleq \frac{\#\text{samples when } \varepsilon > \text{PL}}{\text{Total}\#\text{samples}}$$

The third number is the ratio between the mean protection level at the beginning of the bias sequence and the end of the simulation, r_{PL} (i.e., $r_{\text{PL}} = \text{PL}(t_{\text{end}})/\text{PL}(t_0)$). This number gives an indication of the capacity of the estimator to guarantee an integrity over time. Indeed, if

Fig. 9. Position estimation error comparison for Willsky, AGLR, and MGLR with different elimination methods (SEQ = sequential, GLOBAL = global) for 900 Monte Carlo simulations. The black curves represent the 3σ time sample uncertainty.

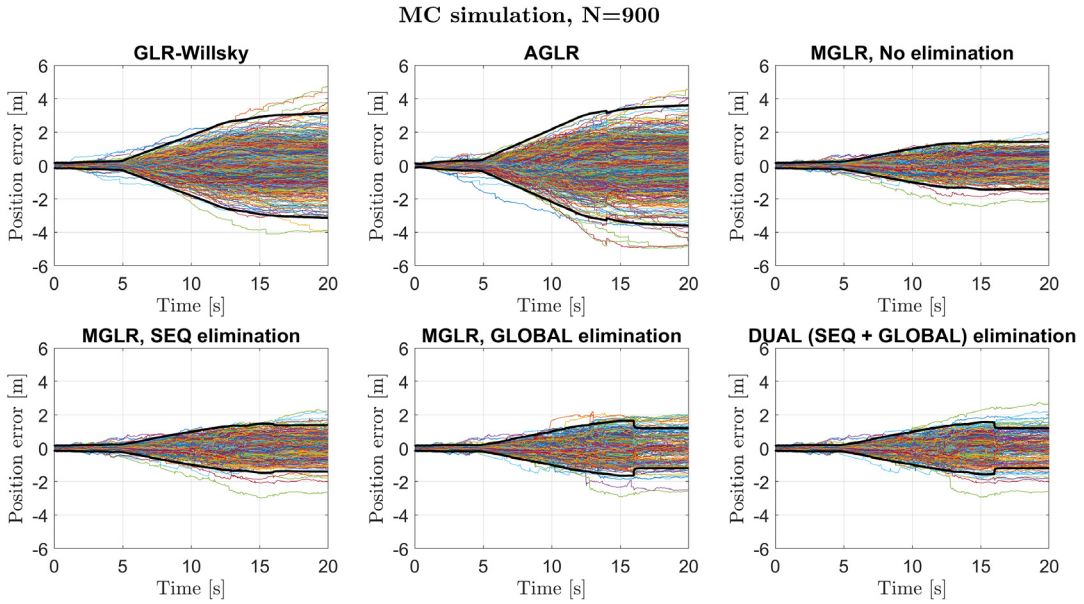

Fig. 10. Protection level comparison for Willsky, AGLR, and MGLR with different elimination methods (SEQ = sequential, GLOBAL = global) for 900 Monte Carlo simulations.

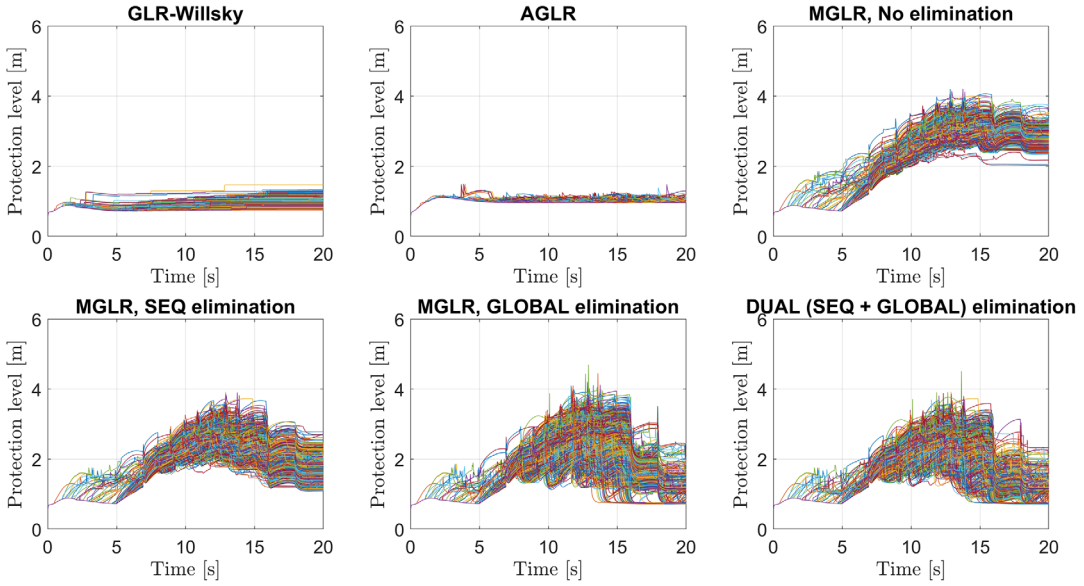

Drone Syst. Appl. Downloaded from cdnsciencepub.com by LINKOPINGS UNIVERSITETSBIBLIOTEK on 09/06/22
For personal use only.

Drone Syst. Appl. Downloaded from cdnsciencepub.com by LINKOPINGS UNIVERSITETSBIBLIOTEK on 09/06/22
For personal use only.

Table 1. Mean of error standard deviations, rate of integrity, and protection level ratio for 900 Monte Carlo simulations.

	$\bar{\sigma}$	r_{int}	r_{PL}
GLR	0.3339	0.1382	1.2971
AGLR	0.3685	0.1383	0.9687
MGLR	0.1889	**0**	3.4644
MGLR-SEQ	**0.1674**	0.0001	2.0099
MGLR-GLOBAL	0.2032	0.0048	1.1514
MGLR-DUAL	0.1737	0.0036	**1.1313**

Note: The lowest (best) values are shown in boldface.

a bias sequence leads to a net increase of the protection level ($r_{\text{PL}} > 1$), the availability of the position estimation from an integrity point of view (PL < AL) will degrade over time.

From the above Monte Carlo batch, we get the results in Table 1.

From the curves and the quantitative results, we can discern three tendencies:

- The MGLR significantly reduces the estimation error over time as compared to the GLR and AGLR algorithms.
- The protection level of the MGLR (all versions) better reflects the evolution of the estimation error during the bias sequence compared to the GLR and the AGLR.
- The bias elimination strategies have a significant impact on the net protection level growth but a marginal impact on the estimation error. The dual elimination is in the example the most promising strategy for reducing the error and the protection level, but this is by no rate a general result.

7. Experimental evaluation

An experimental evaluation using a car-mounted low-cost IMU and GNSS receiver was performed in an urban environment, the city centre of Toulouse, France, to evaluate the MGLR algorithm in a realistic scenario and compare it to the classical GLR (Willsky's GLR) using ad hoc sequential bias detection. The version of the MGLR that is evaluated uses a LS-based re-identification step with global and sequential bias elimination.

7.1. GLR algorithm tuning

The Kalman filter of the GLR algorithms (Willsky's GLR and the MGLR) uses the GNSS position and velocity (Doppler) as output measurements, and the IMU acceleration in the absolute frame as the input. The IMU is sampled at 50 Hz while the GNSS position and velocity are available at 5 Hz (given that four or more satellites are tracked). The GNSS position measurement standard deviations are set to 5/3 m. The standard deviation of the GNSS velocity measurements are set to 1/3 m/s on all axes. The acceleration standard deviation is set to 5/3 m/s^2 on all axes. These values are found by studying the sensor outputs in the absence of a degrading environment.

The GLR detection and observation windows are set to $L = 5$ s and the probability of false alarm is set to $P_{\text{FA}} = 10^{-4}$.

7.2. Evaluation criteria

In this experiment no ground truth is available, and the consistency of the estimation error is therefore unrealistic to assess; however, by post-treating the data with non-causal filtering and filling in the blanks by integrating non-causally de-biased speed measurements, a reference position was obtained. This reference position is used to qualitatively

Fig. 11. GPS measurement error using the reconstructed reference.

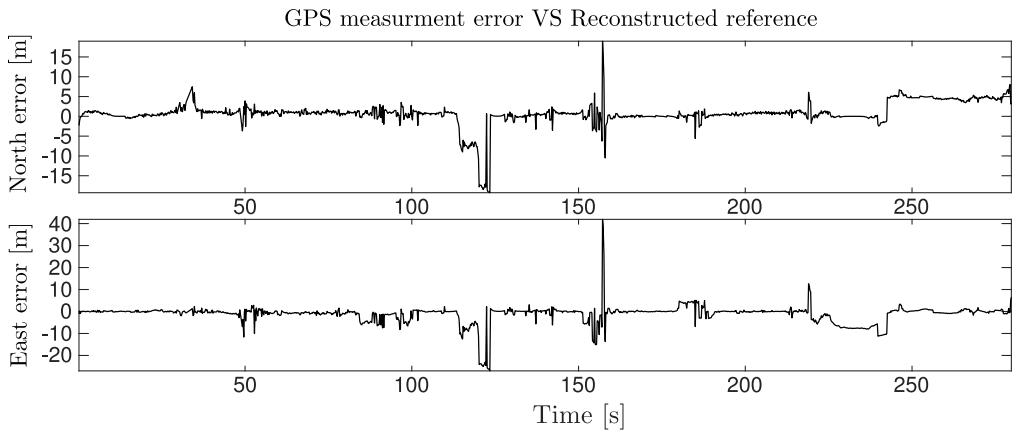

Fig. 12. GPS speed measurements from Doppler shift.

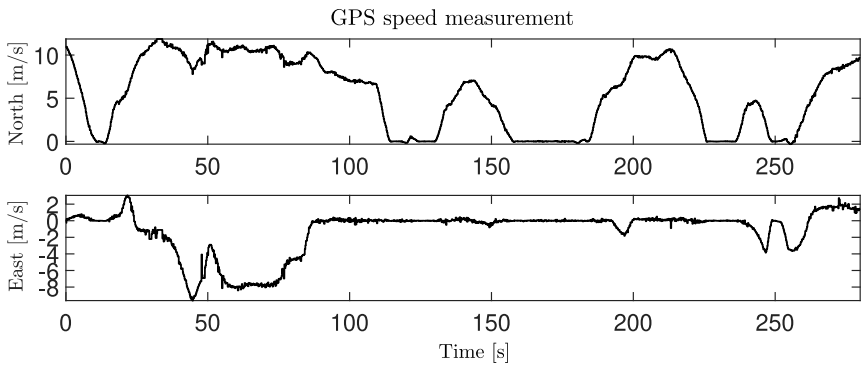

judge whether apparent measurement biases are detected and estimated and whether the bias elimination is effective in identifying absence of bias. The main focus of the evaluation therefore lies on the integrity, which is evaluated through the protection level relative to the alert level.

The alert level is set to 20 m. It can be argued that urban aerial navigation for drones can be compared to a permanent precision approach for an aircraft. In this case, the horizontal (north and east axes) alert limit is 40 m and the vertical (down axis) alert limit is 10–35 m. A general alert level of 20 m therefore seems appropriate.

The experimental results are evaluated according to *accuracy*, *consistency*, and *integrity*, as mentioned in the introduction. Only the results for the north and east axes are shown since the reconstructed ground truth for the down axis was of bad quality.

The GPS position measurement error is shown in Fig. 11. The nature of the faults affecting the GPS are clearly shown: it is a combination of bias jumps followed by drifts, and occasional impulsive noises. The GPS speed measurements, shown in Fig. 12, on the other hand, are not perturbed by the same phenomena as the position and remain healthy throughout the experiment, apart from occasional outliers (e.g., around 50 s).

Drone Syst. Appl. Downloaded from cdnsciencepub.com by LINKOPINGS UNIVERSITETSBIBLIOTEK on 09/06/22
For personal use only.

Fig. 13. Estimation result for Willsky's GLR along the north axis in the urban navigation scenario. Estimation error (black), confidence interval (blue dash-dotted), protection level (green), and alert level (red dashed).

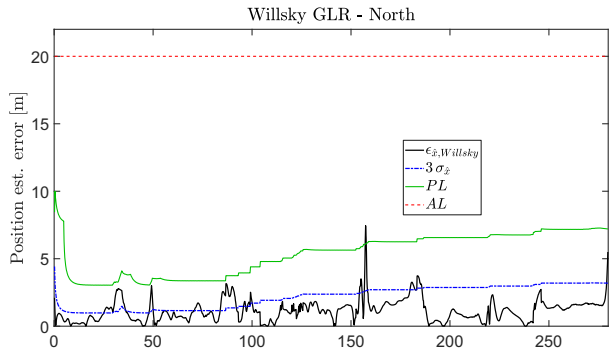

Fig. 14. Estimation result for the MGLR-LS with global and sequential elimination along the north axis. Estimation error (black), confidence interval (blue dash-dotted), protection level (green), and alert level (red dashed).

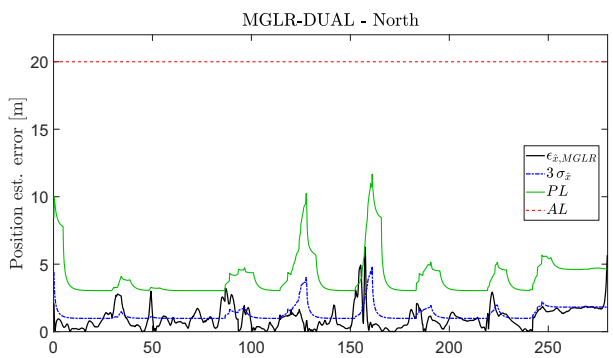

7.3. Estimation along the north axis

Accuracy: The accuracy is similar for Willsky's GLR (see Fig. 13) and the MGLR (see Fig. 14).

Consistency: Overall for both algorithms, the confidence set is badly estimated. The MGLR is slightly better off due to the bias elimination, but the overall consistency is not satisfactory.

Integrity: The protection level is well estimated for the MGLR and overestimated for Willsky's GLR, apart from one occasion around 150 s due to the burst of measurement jumps seen at this occasion in Fig. 11.

7.4. Estimation along the east axis

Accuracy: Both Willsky's GLR (see Fig. 15) and the MGLR (see Fig. 16) have a generally small estimation error. However, Willsky's GLR shows a drift of the confidence interval whereas for the MGLR it is better adapted apart from around the 200 s mark.

Consistency: The consistency is better for Willsky's GLR than the MGLR due to the confidence interval drift described above.

Integrity: Willsky's GLR showcases a typical behaviour where the estimation error remains low, but the protection level increases due to bias detections. The MGLR keeps the integrity of the position estimate throughout the scenario. It can be noted that the bias

Drone Syst. Appl. Downloaded from cdnsciencepub.com by LINKOPINGS UNIVERSITETSBIBLIOTEK on 09/06/22
For personal use only.

Fig. 15. Estimation result for Willsky's GLR along the east axis. Estimation error (black), confidence interval (blue dash-dotted), protection level (green), and alert level (red dashed).

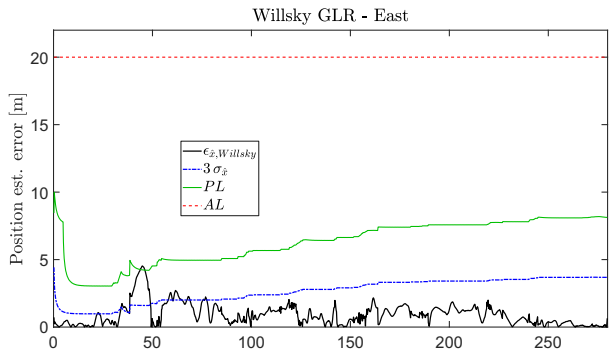

Fig. 16. Estimation result for the MGLR-LS with global and sequential elimination along the east axis. Estimation error (black), confidence interval (blue dash-dotted), protection level (green), and alert level (red dashed).

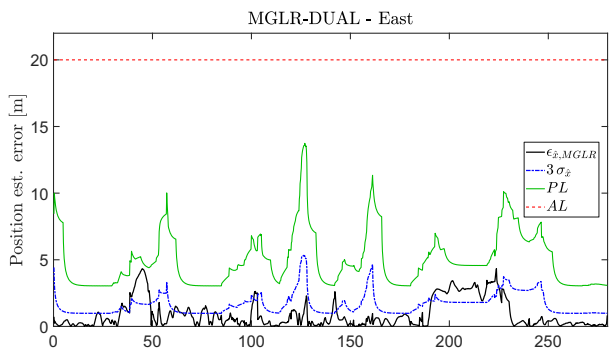

elimination helps keep the protection level near its nominal value in steady state. Note also that the varying height of the protection level peaks for the MGLR, which depends partially on the number of biases currently being estimated.

8. Conclusion and future work

In this paper we have presented the problem of state estimation with non-redundant measurements subject to frequently appearing and disappearing bias jumps intermittent bias. We have proposed an extension of the GLR algorithm, named MGLR, for high-integrity state estimation over time using continuous estimation of detected biases and different bias elimination strategies. The resulting algorithm has been tested against the classical GLR algorithm in a realistic scenario of urban navigation. The objective of the evaluation was to assess the estimation accuracy, the error consistency, and the estimation integrity.

Some general conclusions can be drawn:

- The MGLR reduces the drift of the estimation error as compared to Willsky's GLR when biases appear in a rapid succession or are hidden in noise.
- The re-identification step of the MGLR both serves as a refinement of the bias estimation, and as an improvement of the protection level estimation, which is otherwise truncated.

Drone Syst. Appl. Downloaded from cdnsciencepub.com by LINKOPINGS UNIVERSITETSBIBLIOTEK on 09/06/22
For personal use only.

Drone Syst. Appl. Downloaded from cdnsciencepub.com by LINKOPINGS UNIVERSITETSBIBLIOTEK on 09/06/22
For personal use only.

- The proposed bias elimination works fairly well in most cases and reduces the residual estimation error and protection level over time compared to Willsky's GLR and the AGLR.
- Continuous estimation of bias jumps and their covariance allows proper assessment of the impact of the bias estimation on the integrity of the corrected state. Table 1 clearly indicates that the MGLR (all versions) ensures a significantly higher integrity than the classical GLR and the AGLR.

The major identified drawbacks are:

- The MGLR re-identification step assumes Gaussian noise and is rapidly degraded if this condition is not met, or if the measurement covariance is badly tuned.
- The estimated error covariance post-fault seems to have no physical relevance in the verification of the continued error consistency in the case of faults. It does, however, play a role in the calculation of the protection levels, which seem properly estimated in most cases.
- The MGLR re-identification relies on deterministic fault signatures to identify the bias amplitudes, which is also true for the GLR detector itself. If one has to consider a vast number of different bias shapes (ramp, sinusoidal, sigmoids, etc.) the complexity of the algorithm may be a problem (the complexity increases linearly with the number of fault signatures).

8.1. Future work

The MGLR algorithm, as an extension of the GLR algorithm, points to interest in combining detection and identification to overcome the fundamental problem of measurement biases on non-redundant measurements.

In this paper, it was applied to the case of disturbed GNSS measurements in a complex environment to cancel position jumps. The proposed approach improves the accuracy of the localization and the consistency of uncertainties. This is particularly promising for urban safe navigation (even without redundant measurements) because the protection levels are reliable and do not grow indefinitely as with classical GLR in such a situation. For example, this makes it possible to find a safe path between obstacles that would rapidly lead to no solution with classical GLR due to protection levels becoming too large.

However, the method is still very constrained in terms of noise characteristics and fault signatures, which limits the application domains.

Future work to improve the algorithm, or the class of such algorithms, should address these drawbacks as a priority. For example, one can imagine applying data-driven methods to whiten the innovation signal used by the detector, or simply replace the detector by a data-driven one based on a neural architecture. The re-identification step can be improved in coloured noise cases by replacing the LS estimation by M-estimation (see, e.g., Faurie and Giremus (2010)), or some other iterative optimisation based technique. Alternatively, one could resort to data-driven regression based directly on biased innovation data, a powerful tool for regression with coloured noise (e.g., Brossard et al. (2020)).

Acknowledgements

The authors wish to thank Alexandre Amiez (ONERA) for help with the experimental setup.

Data availability

The experimental data set used to evaluate the algorithm is publicly available at: https://github.com/gustavlundin/pos-est-eval/releases/tag/v1.0 with a permanent DOI link 10.5281/zenodo.6840877.

Drone Syst. Appl. Downloaded from cdnsciencepub.com by LINKOPINGS UNIVERSITETSBIBLIOTEK on 09/06/22
For personal use only.

Contributions

G.Ö.L.: Conceptualization, Methodology, Investigation, Writing; **P.M.**: Conceptualization, Methodology, Writing Review & Editing; **A.M.**: Conceptualization, Methodology, Writing Review & Editing; **G.H.**: Methodology, Writing Review & Editing.

Funding

The authors declare no specific funding for this work.

References

Alcalay, G., Seren, C., Hardier, G., Delporte, M., and Goupil, P. 2018. An adaptive extended Kalman filter for monitoring and estimating key aircraft flight parameters. IFAC-PapersOnLine, **51**(24): 620–627. doi: 10.1016/j.ifacol.2018.09.640.

Brossard, M., Bonnabel, S., and Barrau, A. 2020. Denoising IMU gyroscopes with deep learning for open-loop attitude estimation. IEEE Robot. Automat. Lett. **5**(3): 4796–4803.

Faurie, F., and Giremus, A. 2010. Combining generalized likelihood ratio and M-estimation for the detection/compensation of GPS measurement biases. In Acoustics Speech and Signal Processing (ICASSP), 2010 IEEE International Conference on, IEEE, pp. 4178–4181.

Gao, C., Zhou, H., Wu, R., Xu, X., Shen, F., and Guo, Z. 2016. Parameter estimation and multi-pulse target detection of MIMO radar. In 2016 IEEE Region 10 Conference (TENCON), IEEE, pp. 909–914.

Gustafsson, F. 2000. Adaptive filtering and change detection, 1st ed. Wiley, New York.

Jamouli, H., El Hail, M., and Sauter, D. 2012. A mixed active and passive GLR test for a fault tolerant control system. Int. J. Appl. Math. Comput. Sci. **22**(1): 9–23. doi: 10.2478/v10006-012-0001-1.

Jamouli, H., and Sauter, D. 2008. An active generalized likelihood ratio test in a reconfigurable fault-tolerant control system. In 2008 16th Mediterranean Conference on Control and Automation, IEEE, pp. 1786–1791.

Jiang, C., Chen, Y., Xu, B., Jia, J., Sun, H., Chen, C., et al. 2022. Vector tracking based on factor graph optimization for GNSS NLOS bias estimation and correction. IEEE Internet Things J. doi: 10.1109/JIOT.2022.3150764.

Kerr, T.H. 2006. Drawbacks of residual-based event detectors like GLR or IMM filters in practical situations. In IEEE Transactions on Signal Processing. IEEE.

Lesouple, J., Thierry, R.M.S., Tourneret, J.-Y., and Vi- gneau, W. 2019. Multipath mitigation for GNSS positioning in an urban environment using sparse estimation. IEEE Trans. Intell. Transp. Syst. **20**(4): 1316–1328. doi: 10.1109/TITS.2018.2848461.

Liu, H., and Zhong, M. 2014. A nonlinear version of the generalized likelihood ratio test. In Control Conference (CCC), 2014 33rd Chinese, IEEE, pp. 3175–3180.

Lu, P., Van Eykeren, L., van Kampen, E., de Visser, C.C., and Chu, Q.P. 2015. Adaptive three- step Kalman filter for air data sensor fault detection and diagnosis. J. Guid. Control Dyn, 39(3). doi: 10.2514/1.G001313.

Palmqvist, J. 1996. Integrity monitoring of integrated satellite/inertial navigation systems using the likelihood ratio. Licentiate Thesis. Linköping University.

Pei, Y., Biswas, S., Fussell, D.S., and Pingali, K. 2019. An elementary introduction to Kalman filtering. Commun. ACM, **62**(11): 122–133.

Pirmoradi, F.N., Sassani, F., and De Silva, C.W. 2009. Fault detection and diagnosis in a spacecraft attitude determination system. Acta Astronautica, **65**(5): 710–729.

Van Trees, H.L. 2001. Classical detection and estimation theory. Detection, estimation, and modulation theory, John Wiley & Sons, Ltd., Chap. 2, pp. 19–165. ISBN: 9780471221081. doi: 10.1002/0471221082.ch2.

Willsky, A.S. 1976. A survey of design methods for failure detection in dynamic systems. Automatica, **12**(6): 601–611.

Willsky, A.S., and Jones, H.L.N. 1974. A generalized likelihood ratio approach to state estimation in linear systems subjects to abrupt changes. In 1974 IEEE Conference on Decision and Control including the 13th Symposium on Adaptive Processes. pp. 846–853. doi: 10.1109/CDC.1974.270554.

Xu, L., and Li, J. 2007. Iterative generalized-likelihood ratio test for MIMO radar. IEEE Trans. Signal Process. **55**(6): 2375–2385.

Zhu, N., Marais, J., Bétaille, D., and Berbineau, M. 2018. GNSS position integrity in urban environments: A review of literature. IEEE Trans. Intell. Transp. Syst. **19**(9): 2762–2778.